We thank this Reviewer for thoughtful and constructive comments on our manuscript. We appreciate the time s/he invested in the review. We believe that our revised manuscript addresses all the comments. In this regard, we have revised and rewritten a few sections such as Abstract, method, results, discussion and conclusion in the revised manuscript. Quality control and revision of dissipation estimates, as well as current calculations were also done to ensure the validity of our results. We thought it useful to point out its detailed revisions (lines and sections) in the reply to your comments. Below (highlighted in blue and magenta) is an itemized response to the different issues raised in the review.

Review of "Turbulent dissipation from AMAZOMIX off the Amazon shelf along internal tides paths", by Kouogang et al. Submitted to EGUsphere.

By Kouogang et al.

The paper reports oceanographic observations in the tropical Atlantic ocean within the framework of project AMAZOMIX, which aims to quantify mixing, identify the associated processes, and investigate their impact on nutrient fluxes off the Amazon shelf. The observations were collected during a field campaign in August-October 2021, on board the RV ANTEA with a dedicated satellite coverage (reported elsewhere). The region is well known for large amplitude internal tides and Internal Solitary Waves (ISWs), that were first measured and reported in Brandt et al., 2002, with wave amplitudes exceeding 100 m. Those large amplitude ISWs are clearly seen in Synthetic Aperture Radar (SAR) satellite images, as illustrated in the author's Figure 1. Clearly, the cruise measurements were carefully planned in advance based on the knowledge provided by the SAR image archive. The most relevant aspect reported in the paper is the relative increase of mixing found about 225 km away from two distinct generation sites of internal tidal waves at the shelf break. The site where the relative mixing increases coincides with the surfacing of Internal Tidal (IT) rays emanating from different sites at the shelf break. But it also coincides with the appearance of large amplitude ISWs seen in the satellite record. While the constructive interference of IT rays has been suggested, and indeed is consistent with ocean colour images, in the central region of the Bay of Biscay (Western Europe), this aspect has not been documented elsewhere until now. It is therefore remarkable the association made by the authors between enhanced mixing and IT interference.

Thanks for this very concise and precise summary. We took the liberty of using some of your wording to improve our abstract and our conclusion.

However, a more comprehensive comment should be made concerning the presence of ISWs near Station S14, and its possible relation with the measured increased mixing.

R: This is a very interesting question. We have a specific point on the discussion (in lines 551-569 of the revised manuscript) on that matter, and we agree that this funding is quite important. Please find the revised section "**Discussion on the strong mixing at S14**" below:

“

Discussion on the strong mixing at S14

Along the IT paths, elevated remote dissipation rates (within [10^{-7}, 10^{-6}] W kg^{-1}) were identified ~ 230 km from the shelf-break at S14.

This region is well known for intense IT dissipation, as shown by a realistic model (Tchilibou et al., 2022; Assene et al., 2024), and for the highest occurrences of ISWs generated by ITs (Fig. 1a; de Macedo et al., 2023), with large-amplitude ISWs exceeding 100 m clearly visible in satellite records (Brandt et al., 2002).

At station S14, where relative mixing increases, IT rays surfacing from two distinct IT generation sites coincide with the appearance of ISWs and mark the location where the NBC vanishes.

This region of wave-wave interactions can lead to the constructive interference of IT rays, potentially facilitating the emergence of higher tidal modes (New & Pingree, 1992; Silva et al., 2015; Barbot et al., 2022; Solano et al., 2023). These higher modes, in turn, could enhance the generation of nonlinear ISWs (e.g., Jackson et al., 2012) and contribute to the elevated dissipation rates (Xie et al., 2013), as observed at this station.

Moreover, IT interactions with baroclinic eddies may also contribute to turbulent dissipation (Booth and Kamenkovich, 2008), particularly in this area of pronounced eddy activity. However, no repeated AMAZOMIX stations observed during a tidal period were enclosed by mesoscale eddy activity, except potentially around site E, where possible evidence of a subsurface eddy was detected at S21 (Dossa et al., 2024, in preparation).

Future studies are needed to unravel the intricate interplay among these processes. The data collected during the AMAZOMIX cruise will provide a guide for improving our understanding and advancing parameterizations for modeling studies.

”

This question is so interesting that we are dealing with an additional paper. Indeed, AMAZOMIX provides acoustic data that clearly shows ISW and overturn associated with it at station 14, and a paper is in construction on this matter. Furthermore, their signature at the surface was studied in Macedo et al., 2023 in the region. The mixing hotspots observed at this station could be related to their presence, but more work is needed to establish it with more confidence

The authors calculate the turbulent kinetic energy (TKE) dissipation rates and vertical diffusivities making use of microstructure and hydrography data collected at a series of stations and transects in a vast study region, being able to compare these values within internal tide pathways, and away from those paths. The observations also reveal a great deal of mixing at the shelf break, as expected. **Baroclinic shear currents were calculated from ADCP data collected between stations and transects. It was then possible to estimate the ratio contribution to mixing between IT and Baroclinic Currents (BC). Interestingly, ITs dominate the ratio for IT/BC near the generation sites of ITs at the shelf break (65%/35%) and also at Station S14, 225 km away from the shelf break, admittedly where the IT beams coming from different sites may interfere (60%/40%).** Although this fact is suggestive of the IT rays interference being capable of impacting mixing well away from the shelf break, the authors do not attempt comparison with the impact ISWs alone would have, on mixing.

R: Thank you for your comment.
Indeed, ISWs may influence mixing. While our study did not quantify the specific contribution of ISWs, we suggest that their presence, likely resulting from IT decay, could play a role in the mixing process at S14. In order to explore further the difference between ITs mixing compared to ISWs mixing a non hydrostatic model at very fine resolution should be runned such as in da Silva et al. (2015) and Solano et al. (2023). It would be very interesting to compare the AMAZOMIX data to such model.

The manuscript is reasonably written (with some minor pitfalls indicated below), and the data analysis certainly merits publication at EGUsphere. The hypotheses tested in the paper are well explained and presented, representing a milestone in the oceanography of the study region. The paper also includes an extensive appendix with auxiliary results. This reviewer recommends publication after some minor corrections (please see list below).

Minor comments:

Introduction:

Line 46 – 47: “They can dissipate where the energy beam reflects at the bottom, at the surface or at the thermocline levels…”; The authors start describing bottom reflection of IT beams etc. without first explaining how those beams form and propagate in the vertical. A reader may like to read first how these beams are formed and why they propagate following rays that are determined by the well known formula that gives the angle to the horizontal. There should be a more comprehensive explanation about tidal beams before this point in the text. It may be worth referring to the work of Theo Gerkema (Gerkema, 2001 and Gerkema and Zimmerman, 2008).

R: Thanks for your comments and suggestions. We have rewritten to make it clearer in the text as you suggested. The revisions can be found in lines 34-82, as shown below:

“

1 Introduction

Turbulent mixing in the ocean plays an important role in sustaining the thermohaline and meridional overturning circulation and in closing the global ocean energy budget (Kunze, 2017). These processes have strong implications for the climate, influencing heat and carbon transport, as well as nutrients supply for photosynthesis (Huthnance, 1995; Munk and Wunsch, 1998). Mixing processes can result from wind in the surface waters layer, internal waves and shear instability in the ocean interior, and bottom friction near the bottom layer (Miles, 1961; Thorpe, 2018; Ivey et al., 2020; Inall et al., 2021). Barotropic tides interacting with steep shelf-break topography trigger internal waves at tidal frequencies and harmonics, known as internal tides (ITs), which can propagate and produce mixing. These ITs can be expressed by large vertical displacements (up to tens of meters) of water masses (Garrett and Kunze, 2007). After their generation on the shelf-break, the (more unstable) higher modes of ITs may dissipate locally, while the lower modes can propagate far away (Zhao et al., 2016). IT beams (generated where the slope of the ITs and the topography match together on the shelf-break) can propagate vertically, resulting in reflection, scattering and dissipation of ITs at the bottom, surface waters, or thermocline

levels (New and Da Silva, 2002; Gerkema and Zimmerman, 2008; Bordois, 2015; Zhao et al. 2016). They can also dissipate when energy fluxes interfere (Zhao et al., 2012) or interact with strong baroclinic eddies or currents (Rainville and Pinkel, 2006; Whalen et al., 2012). Furthermore, ITs may disintegrate into packets of higher-mode nonlinear internal solitary waves (ISWs), which can propagate and dissipate offshore (Jackson et al., 2012).

Previous and recent studies have shown that ITs-induced turbulent mixing can affect the surface, such as sea surface temperature (Ray and Susanto, 2016; Nugroho et al., 2018; Assene et al., 2024), chlorophyll content (Muacho et al., 2014; M'Hamdi et al., 2024; in preparation), marine ecosystems (Wang et al., 2007; Zaron et al., 2023), and atmospheric convection and the rainfall structure (Koch-Larrouy et al., 2010, Sprintall et al. 2014).

In the western tropical Atlantic, the Amazon River-Ocean Continuum (AROC) constitutes a key region of the global oceanic and climate system (Araujo et al., 2017; Varona et al., 2018). This region (Fig. 1a) is characterized by a system of western boundary currents, including North Brazil Current (NBC). NBC, which flows northwestward, has its core velocities (~ 1.2 m s^{-1}) that remain stable from the surface to a depth of 100 m (Johns et al., 1998; Bourlès et al., 1999; Barnier et al., 2001; Neto and Silva, 2014). This region also experiences highly variable dynamics due to the Amazon River Plume. During the rainy season (May-July), peak discharge can extend the plume over 1500 km offshore, northwest along the NBC. In the dry season (September-November), reduced discharge and stronger saline intrusion may confine the plume to less than 500 km offshore, near the Amazon Shelf, with some eastward dispersion (Coles et al., 2013). The Amazon plume can generate vertical shear in underlying currents, enhancing mixing. Additionally, a system of Amazonian Lenses of water (AWL), influenced by continental inputs, may affect both the boundary layer and mixed layer patterns (Silva et al., 2005; Prestes et al., 2018).

In the AROC region, the Amazon shelf-break is a hotspot for the generation, propagation and dissipation of ITs and ISWs as a result of non-linear processes (Geyer, 1995; Brandt et al., 2002; Magalhães et al., 2016; Ruault et al., 2020; Tchilibou et al., 2022; Fig 1). Previous studies using Synthetic Aperture Radar (SAR) satellite images (Magalhaes et al., 2016) identified ISWs along the path of ITs propagating from two sites (i.e., sites Aa and Ab; Fig. 1a). Conversely, other sites showed no ISWs propagation (i.e., sites E and D; Fig. 1a, 1b and 1c) (see Magalhaes et al., 2016 for definition). Using numerical modeling, Tchilibou et al. (2022) showed that about 30 % of the M2 (dominant tidal component; Le Bars et al. 2010) ITs energy is dissipated locally (for higher-modes ITs) at sites E, Aa, Ab and D (Fig. 1a), while the remaining lower-modes ITs energy can be dissipated remotely. Dissipation away from the generation sites (E, Aa, Ab and D; Fig. 1a) can result from the shear instabilities caused by ITs-ITs and/or ITseddy/current interactions. Despite the presence of ITs, no direct measurements of dissipation rates have been conducted to our knowledge.

The mixing induced by these internal waves in the region was observed during the AMAZOMIX cruise (Bertrand et al., 2021). The cruise was designed with stations/transects inside and outside ITs fields (Fig. 1a and 1c) to measure ITs dissipation and study their impact on the AROC ecosystem. Direct microstructure measurements of temperature, salinity and velocity were conducted at the different repeated stations/transects over a M2 tidal cycle (~ 12.42 h). These cruise measurements offer an opportunity to explore whether ITs play a role in mixing within the AROC region. In this study, we will quantify mixing and identify the associated processes off the Amazon shelf. We will calculate turbulent kinetic energy (TKE) dissipation rates, vertical displacements of isopycnal surfaces and vertical eddy diffusivities using in situ microstructure and hydrography

data. Finally, the baroclinic shear of currents and their contributions to mixing will be calculated from current data collected between stations and transects.

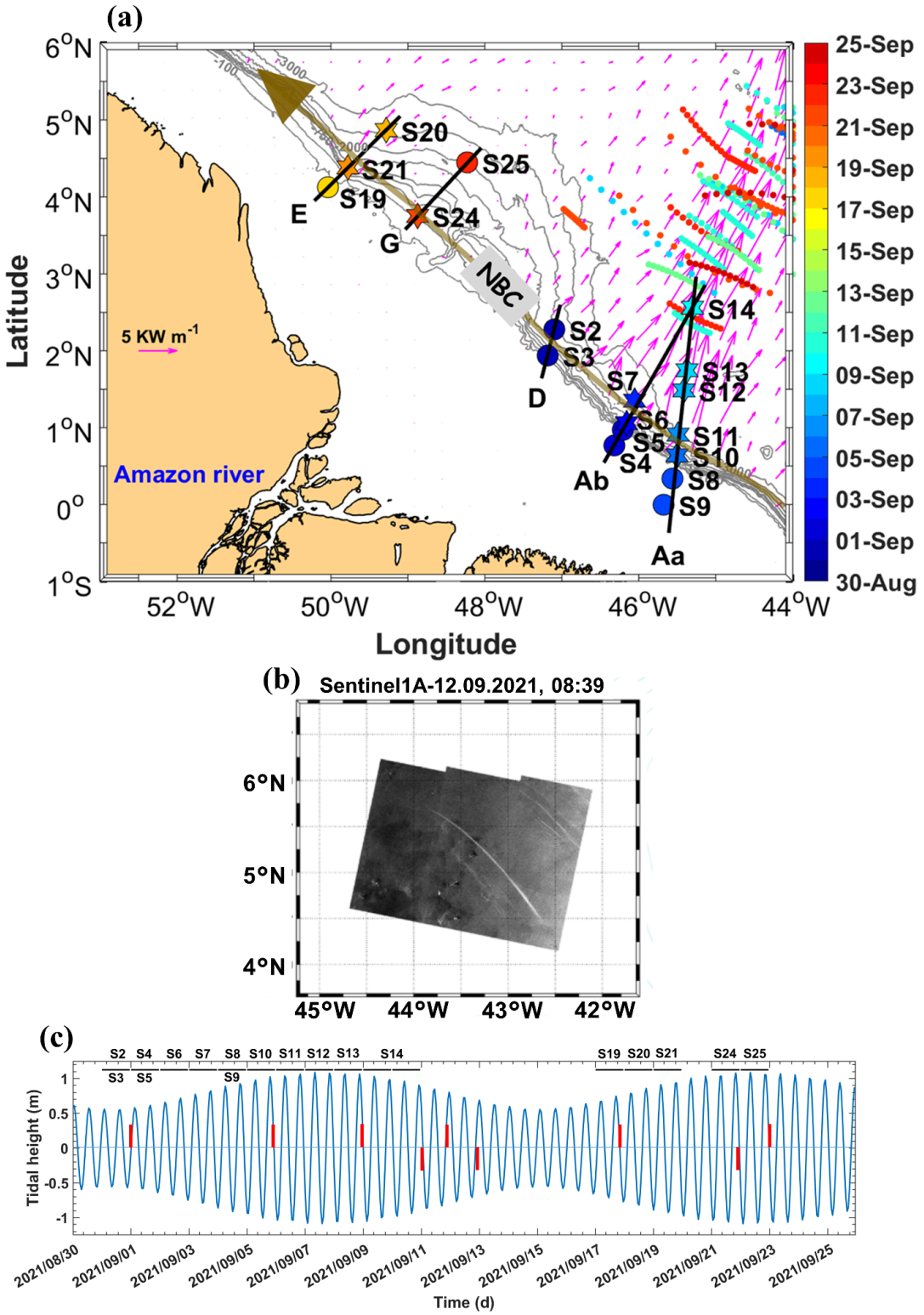

Figure 1: a) Map of a part of the AMAZOMIX 2021 cruise off the Amazon shelf, showing bathymetric contours (100 m, 750 m, and 3000 m isobaths) in gray. Colored circles and stars indicate short and long CTD-O2/L-S-ADCP stations, respectively, with the corresponding sampling dates represented by the color bar. Solid black lines depict SADCP transects (for Aa, Ab, D, G, and E). Magenta arrows show the 25-hour mean

depth-integrated baroclinic IT energy flux (September 2015, from the NEMO model) originating from IT generation sites (Aa, Ab, D, and E) along the shelf break. The solid brown line represents the NBC pathways illustrating background circulation. Shattered colored lines highlight ISW signatures. b) 1A Sentinel image acquired on 12th September 2021, showing ISW signatures. c) Tidal range at AMAZOMIX stations, with ISW signature dates marked by red bars.

"

Line 53: The reference Muacho et al, 2014 should be referred earlier, together with M'Hamdi et al., 2024, in preparation)

R: Thanks for your suggestions. We have rewritten to make it clearer in the text as you suggested. The revisions can be found in lines 51-52 of the revised manuscript, as shown in your previous comment.

Line 62: Please include reference Brandt et al., 2002 in JPO about ISW in situ observations.

R: we could not find this reference in JPO. Could you please share the link to this article, if you have it ?.

Line 69: "…no direct measurements of dissipation rates have been conducted.". Do you mean before the present paper?

R: We have corrected the sentence of the text in lines 72-73 of the revised manuscript. I meant that:

"

Despite the presence of ITs, no direct measurements of dissipation rates have been conducted to our knowledge.

"

Methods:

Line 170: "…time series with LADCP profiles glued below ~500m…". later, in line 209 (page 8), the word "stitched" is used with a similar meaning? Could the authors use jargon more carefully, and consistently, please.

R: Thanks for your remarks. We have rewritten to make it clearer as you suggested in lines 122-235 of the revised manuscript. The revision of section "methods" can be found below:

"

2.2 Methods

TKE dissipation rates

The VMP data are processed using ODAS Matlab library (developed by Rockland Scientific International, Inc) to infer the TKE dissipation rate (ε). The processing methods for the VMP data are briefly described here and adhere to the recommendations of ATOMIX (Analyzing ocean turbulence observations to quantify mixing), as

reported by Lueck et al. (2024), and have been validated against the benchmark estimates (presented in Fer et al., 2024).

First, the VMP data are converted into physical shear units, and the time series are prepared. Continuous sections of the time series are selected for dissipation estimation. Before spectral estimation, the aberrant shear signals caused by vessel wake contamination are removed. Collisions of the shear probe with plankton and other particles are removed using the de-spiking routine. The records from each section are then high-pass filtered (e.g., at station S6 and S10; Fig. 2a, and Fig. A1, Appendix).

Shear spectra are estimated using record lengths (L) and Fast Fourier Transform segments of 2 s, which are cosine windowed and overlapped by 50% (e.g., at station S6 and S10; Fig. 2b, and Fig. A1, Appendix). Additionally, vibration-coherent noise is removed. Different L and overlap (O) settings were selected and tested based on the environment (e.g., deep vs. shallow water), following Fer et al. (2024). For shallow stations, L (O) was shortened to 5 s (2.5 s), in contrast to the 8 s (4 s) used for deeper stations, due to evidence of overturns observed in AMAZOMIX acoustic measurements at deeper stations (Koch-Larrouy et al., 2024; in preparation). This adjustment helped to optimize the spatial resolution of dissipation estimates in shallow water stations.

Finally, ε is determined using the spectral integration method and by comparison with the Nasmyth empirical spectrum (Nasmyth, 1970). Quality assurance tests are carried out in accordance with ATOMIX's recommendations (Lueck et al., 2024). A figure of merit < 1.4 is used to exclude bad data (e.g., at station S6 and S10; Fig. 2b, and Fig. A1, Appendix), and the fraction of data affected by de-spiking is < 0.05.

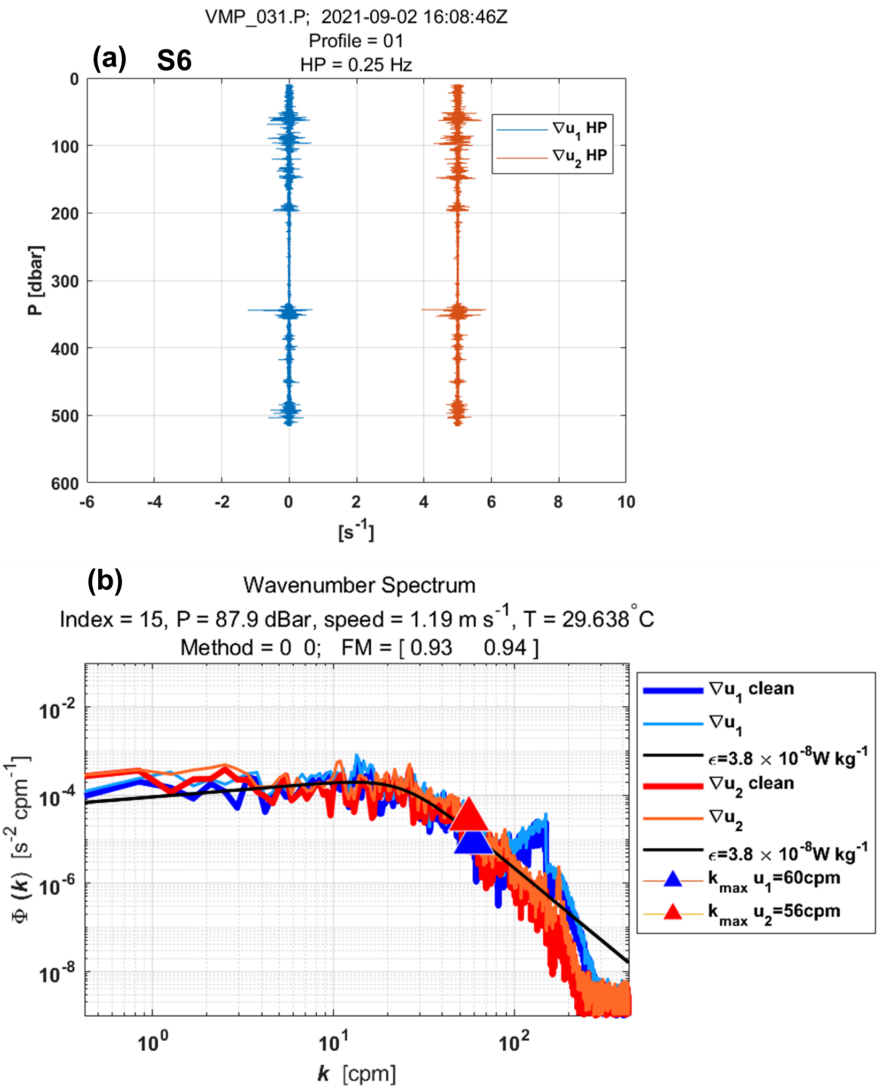

Figure 2: Example of wavenumber spectra from a dissipation structure segment used to determine the dissipation rate at station S6 at a pressure of 87.9 dBar. (a) Cleaned and high-pass filtered signals from shear probe 1 (blue) and shear probe 2 (red, offset by 5 s^{-1}). (b) Wavenumber spectra for shear probes 1 and 2. Thick lines (blue for probe 1, red for probe 2) show shear spectra with coherent noise correction, while thin lines (sky blue for probe 1, orange for probe 2) show spectra without correction. Triangles mark the maximum wavenumber used for dissipation rate estimation. Black lines represent Nasmyth reference spectra for estimated dissipation rate of 3.8 x 10^{-8} W kg^{-1} for both shear probes. Dissipation rate estimates for shear probe 1 and shear probe 2 at a pressure of 87.9 dBar yielded a figure of merit of 0.93 and 0.94, respectively.

The vertical eddy diffusivity coefficient

The efficiency of turbulence in redistributing energy is assessed through the calculation of the vertical eddy diffusivity coefficient (K_z). This coefficient is particularly significant in regions such as pycnoclines, where stratification suppresses mixing, making turbulence-driven mixing a key mechanism for vertical energy transport (Thorpe, 2007).

K_z is calculated from ε following the formulation of Osborn (1980), given by $K_z = \varepsilon\ \Gamma\ N^{-2}$. Here, N^2 is the buoyancy frequency squared, which is calculated using the sorted potential density profiles (σ_θ) obtained from CTD-O_2 data. It is given by $N^2 = -(g/\rho_0)(d\sigma_\theta/dz)$, where ρ_0 is a reference density (1025 kg m^{-3}) and g is the gravitational acceleration. Γ is the mixing efficiency, defined as the ratio between the buoyancy flux and the energy dissipation, and is typically set to 0.2, which corresponds to the critical Richardson number Ri = 0.17 (Osborn, 1980). ε is linearly interpolated into the depths of N^2.

Turbulence within the pycnocline can reduce stratification and increase vertical eddy diffusivity below the mixing layer (Thorpe, 2007). Subsurface mixing, driven by the breaking of ITs and shear instabilities, plays a particularly important role below the mixed layer, especially in equatorial waters (Gregg et al., 2003).

There are several criteria for defining the Mixed Layer Depth (MLD). In this study, we use the commonly accepted density threshold criterion of 0.03 kg m^{-3}, as defined by de Boyer Montégut et al. (2004) and Sutherland et al. (2014), to estimate the MLD for each CTD-O_2 profile. Notably, comparisons with density thresholds of 0.01 and 0.02 kg m^{-3} revealed no major differences in MLD across the AMAZOMIX stations and transects (Fig. A2, Appendix).

The miXing Layer Depth (XLD) is defined as the depth at which ε decreases to a background level (Sutherland et al., 2014). Previous studies have applied various thresholds for background dissipation levels, such as such as 10^{-8} and 10^{-9} W kg^{-1} in higher latitudes based on in situ observations (Sutherland et al., 2014; Lozovatsky et al., 2006; Cisewski et al., 2008; Brainerd and Gregg, 1995) and 10^{-5} m^2 s^{-1} using an ocean general circulation model (Noh and Lee, 2008). In this study, XLD is specified as the depth where ε drops from its first minimum value. This aligns with previous dissipation thresholds and ensures that mixing is captured independently of surface influences. The Upper (UTD) and Lower (LTD/LPD) Thermocline/Pycnocline Depth are delimited as defined by Assunçao et al (2020). UTD corresponded to the depth where the vertical temperature gradient $\partial\theta/\partial z$ = 0.1 ℃ m^{-1}, while LTD/LPD were the last depth below the UTD at which $N^2 \geq 10^{-4}$ s^{-2}.

Baroclinic currents

To analyze the processes explaining dissipation and mixing, particularly along internal tidal (IT) paths, we estimate shear instabilities associated with the semi-diurnal (M2) ITs and mean circulation, as well as their contributions to mixing.

The M2 tidal component of the tidal current is derived by calculating the baroclinic (semi-diurnal) tidal velocity $[u'', v'']$ (Fig. A3, Appendix), following these equations:

$$[u', v'] = [u, v] - [u_{bt}, v_{bt}], \quad (1)$$

$$[u_{bt}, v_{bt}] = \frac{1}{H}\int_{-H}^{0} [u, v]dz, \quad (2)$$

$$[u'', v''] = [u', v'] - [\overline{u'}, \overline{v'}]. \quad (3)$$

Here, $[u, v]$ represent total horizontal velocities (Fig. A3, Appendix) obtained from SADCP data. The components $[u', v']$ and $[u_{bt}, v_{bt}]$ represent baroclinic and barotropic components of horizontal velocities, respectively (Fig. A3, Appendix). H is water depth. The baroclinic mean velocities $[\overline{u'}, \overline{v'}]$ (Fig. A3, Appendix),

calculated to estimate mean circulation along IT paths, are decomposed into along-shore $\overline{u'}_l$ and cross-shore $\overline{u'}_c$ velocities. The overbar denotes the average over a M2 tidal period.

Note that continuously collected SADCP for some stations (e.g., S11) are not sufficiently resolved due to gaps filled by interpolating between time points. The similar processing are applied to the CTD-O_2 data collected alternately. SADCP time series data are less than 17 hours at all long stations, except for S14, which spans 42 hours. As a result, the diurnal and semidiurnal period fittings are not formally distinct (except at S14; Figs. A4 and A5, Appendix), and the inertial period (at least 5 days) cannot be resolved in our dataset. This limits our ability to separate currents by frequency and examine the associated dissipation.

The velocity profiles from LADCP are glued into our SADCP time series data below ~ 500 m depth at long stations.

To evaluate shear instabilities associated with ITs and the mean background circulation, we compute the baroclinic tidal vertical shear squared ($S^{2''}$) and mean shear squared ($\overline{S^{2'}}$) (Fig. A3, Appendix), as follows:

$$S^{2''} = (\partial u''/\partial z)^2 + (\partial v''/\partial z)^2, \quad (4)$$

$$\overline{S^{2'}} = (\partial \overline{u'}/\partial z)^2 + (\partial \overline{v'}/\partial z)^2. \quad (5)$$

To evaluate the impact of bottom friction on mixing, we calculate kinetic energy $\varepsilon_f = \frac{1}{2}\rho_s(u_f^2)$ near the bottom boundary layer at shallow stations using friction velocity $u_f = u_b\sqrt{C_d}$, where C_d=2.5 x 10^{-3} is a drag coefficient obtained from the NEMO model. Huang et al. (2019) showed that the bottom boundary layer thickness spatially varies between 15-123 m in the Atlantic Ocean, with a median of ~ 30-40 m in the North Atlantic. We define bottom layer thicknesses in our study area based on measured bathymetry from CTD-O_2 and near-bottom currents from ADCP. Here, u_b is the total velocity averaged over a thickness of 20 m above the seabed for shallow stations and 40 m for deep stations.

The individual contributions of semi-diurnal ITs and mean circulation are then expressed as follows: $E''/(\overline{E'} + E'')$ for tidal contribution and $\overline{E'}/(\overline{E'} + E'')$ for mean circulation contribution. Here, $E = N^2S$. N is the buoyancy frequency and S is vertical shear. S can be substituted by $S^{2''}$ and $\overline{S^{2'}}$.

Ray tracing calculation

Analyzing both the mean currents and the spatial dimension along the IT pathways offers another insight into the mechanisms responsible for observed mixing (Rainville and Pinkel, 2006). IT energy rays are generated in regions with steep topography, such as the shelf break, where IT slope matches with the bottom slope (i.e., critical slopes) before propagating within the ocean interior. These rays, moving both downward and upward, encounter the seasonal pycnocline, resulting in beam scattering and the formation of large IT oscillations. As these oscillations steepen, they disintegrate into nonlinear ISWs, a process known as "local generation" of ISWs (New and Pingree, 1992). To explore IT paths, ray-tracing techniques are employed, as previously used by New and Da Silva (2002) and Muacho et al. (2014), to investigate the effectiveness and expected pathways of the IT beams off the Amazon shelf. One main assumption in our linear-theory-based hypothesis is that stratification

remains horizontally uniform along the IT propagation path, although in reality, it may vary due to submesoscale and mesoscale variability. This limitation makes the ray tracing approach less realistic but still useful as a first-order estimate of energy distribution. The IT ray-tracing calculation assumes that in a continuously stratified fluid, ITs energy can be described by characteristic pathways of beams (or rays) with a slope c to the horizontal:

$$c = \pm\left(\frac{\sigma^2 - f^2}{N^2 - \sigma^2}\right)^{1/2}, \quad (6)$$

where σ is the M2 tidal frequency (1.4052×10^{-4} rad s^{-1}), and f is the Coriolis parameter. N^2 are obtained from time-averaged AMAZOMIX CTD-O_2, glued with monthly N^2 profiles from Amazon36 (NEMO model outputs, 2012-2016) below 1000 m depth. Amazon36 is a NEMO configuration, specifically designed to cover the western tropical Atlantic from the mouth of the Amazon River to the open sea (see Tchilibou et al., 2022; Assene et al., 2024; for configuration details and model description). IT ray-tracing diagrams are performed along the transects. Seasonal sensitivity tests of rays (August, September, October, and April) are conducted by varying the critical slope positions and N^2 to explore its influence and generate a set of ray paths consistent with characteristics of IT pathways (Figs. A6 and A7, Appendix).

”

Line 174: “… with overbar the average…”. A word seems to be missing between “overbar” and “the average”.

R: Thanks for your remarks. We have rewritten it in line 190 of the revised manuscript, as shown in your previous comment.

Line 183: “… for M2 semi-diurnal baroclinic energy)…”. The parenthesis after the word “energy” appears to be unnecessary!

R: Thanks for your remarks. We have rewritten the subsection “Baroclinic currents” in lines 179-213 of the revised manuscript, as shown in your previous comment.

Line 187: “Previous study of Huang et al. (2019) shown…”. Please revise grammar.

R: Thanks for your remarks. We have revised grammar in lines 207-208 of the revised manuscript, as shown in your previous comment.

Line 188: “… between 15-123 m in Ocean Atlantic”. Do you mean “Atlantic Ocean”?

R: Yes, thanks for your remarks. We have rewritten it in line 207 of the revised manuscript, as shown in your previous comment.

Line 209: “ and stitched…”. Please be consistent with jargon language.

R: Thanks for your remarks. We have rewritten it in line 198 of the revised manuscript, as shown in previous replies.

Results:

Line 218: "… . They are thicker along the IN-ITs…". If you are referring to the "step-like" structures from the previous line, consider using another word for "thicker", e.g. "larger".

R: Thanks for your remarks. We have rewritten it in lines 239-252 of the revised manuscript. The revision of section "Results" can be found below:

"

3.1.1 Thermohaline and IT features

In this subsection, we analyze the density profiles to gain insight into mixing processes and/or wave propagation. Step-like features are observed in the density profiles (Figs. 3a and 3b). During the M2 tidal period, step-like structures ~20-40 m in length occur at depths ranging from 80 to 160 m at stations S10, S12, S13, and S14 (Fig. 3a). These features are more pronounced along the IN-ITs transect Aa and Ab compared to the other transects (e.g., E and G; Figs. A8.a and A8.b, Appendix).

In this layer (between 60 and 170 m depth), significant vertical displacements, ranging from 20 to 60 m, are detected along transects Aa, Ab, and E (e.g., 40 m at S10, 48 m at S6, 52 m at S13, and 32 m at S14; Figs. 3a and 3b). The smallest displacements (~8 m at S25) are observed along the OUT-ITs transect G (Fig. A8.b, Appendix). These vertical displacements are also evident in the variability of the mixed layer depth (MLD), which fluctuates between 18 and 84 m over a semi-diurnal cycle (figure not shown).

In conclusion, the presence of step-like structures and isopycnal displacements suggests strong mixing in the water column, and supports the hypothesis of ITs propagating, with stronger energy along transects Aa and Ab, weaker energy along D and E, and almost absent along G (Fig. 1a).

"

In Figure 3 the choice of colours for dissipation rates (epsilon) is somewhat difficult to grasp. The colours "red" and "magenta" are sometimes confusing, particularly in the vertical profiles in Figs. 3b to 3e. Could the "red" colour be changed to a "light Orange", or similar?

R: Thank you for your comments and suggestions. The light orange color was already used in Figure 3 (as shown below for example) and is sometimes referenced in subsequent figures for analysis. We have changed the magenta color to purple to enhance visual clarity and make it more noticeable.

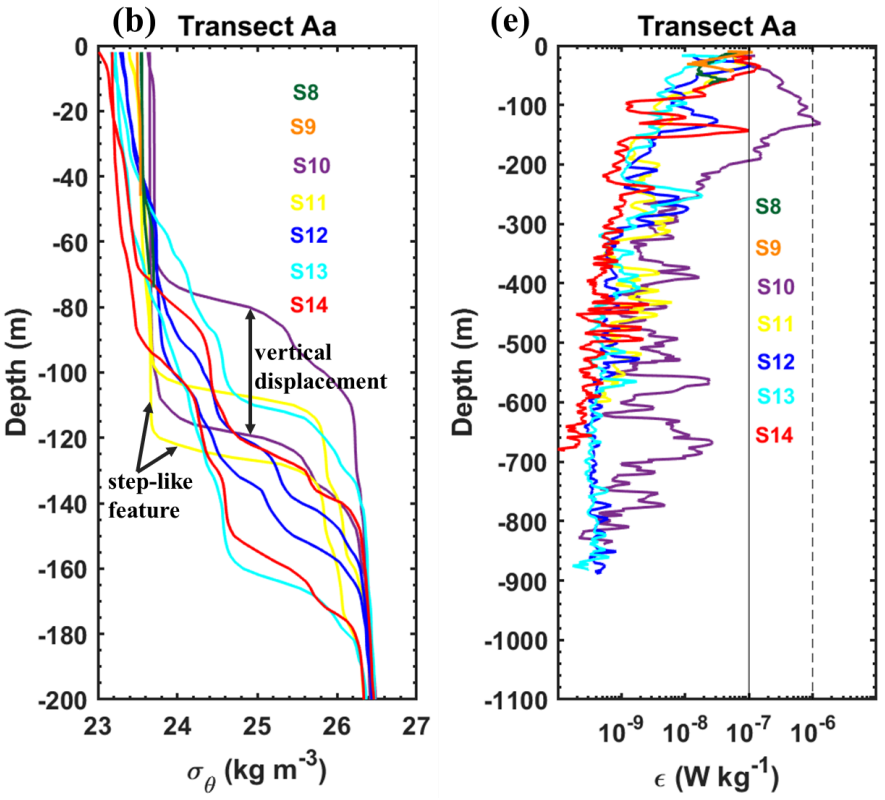

Figure RC3.1: *(b) Density profiles (σ_θ, kg m^{-3}) obtained from CTD-O_2 measurements during the AMAZOMIX 2021 cruise for stations S8 to S14 along transects Aa, located within IT fields. For long stations (S10-S14), two density profiles are shown to highlight step-like structures and isopycnal vertical displacements (illustrated by black arrows) along the transects. Distinct colors are used to represent each station within each transect. The density values for stations S8, and S9 range between 23.4 and 23.8 kg m^{-3}. (e) Vertical dissipation profiles for stations along transects Aa. Distinct colors are used to represent each station within each transect. Dashed and solid black lines in panel (e) are included for comparison purposes.*

Line 236: “Now, ….”; Unnecessary use of word “Now”.

R: Thanks for your remarks. We have rewritten it in line 261 of the revised manuscript.

Line 246: “….are found almost anywhere at S14…”; is there a better word than “anywhere” to be used in this sentence. Perhaps the words “at any depth” would be more appropriate?

R: Thanks for your remarks. We have rewritten it in lines 260-288 of the revised manuscript.

Line 247: “…shelf stations in the ITs regions, S3 and S5, ….” ; the vertical profile of station S3 does not appear in Fig. 3. (it appears only in Fig. A1.c). Please refer to where it appears.

R: Thanks for your remarks. We have rewritten it in lines 275-277 of the revised manuscript, as shown below:

“

For shelf/shallow stations within the ITs regions (S3 and S5; Fig. 4c, and Fig. A8.c, Appendix), mixing is more pronounced, between [10^{-6}, 10^{-5}] W kg^{-1}, near the bottom layer.

“.

Line 271: “… dissipation rates (epsilon) already presented in section 3.1.2, IS….”; do you mean “ARE also reported in Fig. 3”?

R: Yes, thanks for your remarks. We have rewritten it in lines 316-317 of the revised manuscript, as reported here:

“

Dissipation rates, previously presented in subsection 3.1.2 and shown in Fig. 4, are found to be 2-3 orders of magnitude higher in the pycnocline compared at greater depths.

“

In Figure 4b, the baroclinic tidal currents at S11 are less clear. Do you have any reason to suggest for this fact?

R: Thanks for your remarks.
This issue could be related to the temporal interpolation of the SADCP data. Continuous SADCP measurements revealed missing values (e.g., between 13:30 and 15:30) at S11. Interpolation allowed us to estimate current data corresponding to the dissipation times.

Line 287: “Now, …”; Unnecessary use of word “Now”.

R: Thanks for your remarks. We have rewritten it in line 336 of the revised manuscript.

Line 331: “IT ray paths were observed reflecting at the surface….”; The words “were observed” are not the best choice here, as you are talking about a model calculation; This reviewer suggests the use of the words “are expected to reflect” or “were predicted to reflect”.

R: Thanks for your remarks. We have rewritten it in lines 408-409 of the revised manuscript, as shown below:
“

After bottom reflection and subsequent interaction with the pycnocline, the rays are expected to reflect seaward at the surface, typically at distances between 115-400 km.

“.

Line 335: “flow becomes unstable beyond ….”; use the word “below” or beneath” instead of beyond?

R: Thanks for your remarks. We have rewritten it in lines 412-416 of the revised manuscript.

Line 336: “Large epsilon are encountered where IT rays presumably interfere between them or….”

This reviewer does not see “IT ray path interference, since the different ray tracing computations (in red and blue colours) are a matter of different stratification choices, and hence you either have a “blue” ray or a “red” ray.

R: Thanks for your comments.
Our IT interference hypothesis is based on ray-tracing calculations using various stratification scenarios and sensitivity tests, which revealed a packet of rays (see Fig. A19 of paper, Appendix, for example) as shown below in figure RC3.2. To explain the persistent high mixing observed at S14 in the open ocean, we also proposed constructive interference of IT rays originating from two generation sites, Aa and Ab, as discussed in lines 551-569 of the revised manuscript. This hypothesis will be further investigated in a subsequent study.

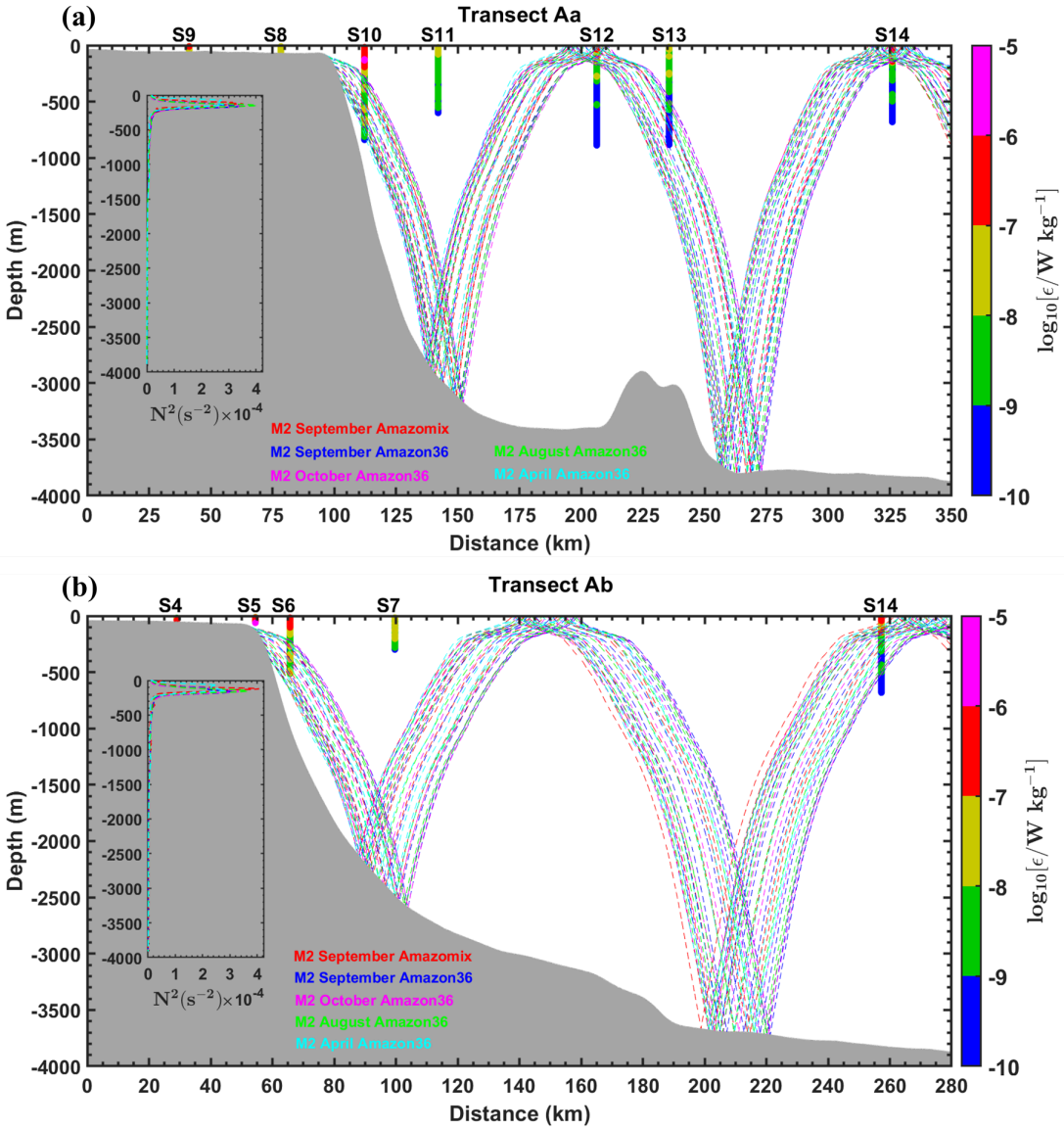

Figure RC3.2: *Sensitivity tests of M2 IT ray-tracing along the transects (a) Aa and (b) Ab, conducted by varying the location of the critical topography slope. The tests use mean buoyancy frequency squared (N^2, in s^{-2}) obtained from CTD-O_2 data (September 2021) and NEMO-Amazon36 model data (2012-2016). Dashed colored lines represent IT beams calculated for different seasons (April, August, October, and September) and for varying locations of the critical topography slope. Grey areas indicate local topography. Panels (a) and (b) also include dissipation rate profiles (ε, in W kg^{-1}, shown as vertical colored bars on a logarithmic scale) from the VMP measurements. Subpanels within each panel illustrate the N^2 profiles derived from AMAZOMIX and the NEMO-Amazon36 model, which were used in the ray-tracing calculations. For comparison, sensitivity tests using N^2 measurements from individual stations along the corresponding transect (e.g., at S10) revealed similar ray paths (not shown), consistent with the packet of rays obtained using the mean N^2.*

Line 338-339: “Some large epsilon are observed where IT rays radiated at the surface (e.g. at S12, S14 and S20)…..”; Large epsilon values are a common feature to all turbulence

profiles of dissipation rates near the surface. It looks more like the effect of wind mixing, rather than surfacing and reflection of IT rays.

R: Thanks for your comments.
Indeed, the mixing on the surface would also be linked to the effect of the wind.
Our study focuses more on the mixing observed outside of surface influence along IT paths, and the contribution of IT compared to other processes.

Line 353: “The next steps of our study IS…”; either use singular (“step”) or use correct tense (“ARE”).

R: Thanks for your remarks. We have rewritten it.
Ultimately, we decided to remove and reserve all sections on “Nutrients fluxes” for a separate paper in progress.

Discussion and Conclusion.

Line 398: “…., both large (up to 60 m length) isopycnal displacements…”; perhaps the wording “…, both large (up to 60 m) AMPLITUDE isopycnal displacements…” is more apropriate?

R: Yes. Thanks for your remarks. We have rewritten it in line 449 of the revised manuscript.

Revisions of section “Discussion and Conclusion” can be found below:

.
“

4 Discussion and Conclusion

The AMAZOMIX 2021 cruise provided, to the best of our knowledge, for the first time, direct measurements of turbulent dissipation using a velocity microstructure profiler (VMP) at multiple stations both inside and outside the influence of ITs. These measurements enabled the study of mixing processes at the Amazon Shelf break and the adjacent open ocean. To capture a full tidal cycle, data on turbulent dissipation rates, hydrography, and currents were collected alternately over 12 hours, with 4 to 5 profiles taken per station (see section 2). The locations of the 12-hour sampling stations were selected based on modeling results that provided realistic maps of IT generation and propagation (Fig. 1a; Tchilibou et al., 2022). Stations were located in the most energetic regions of IT, specifically at sites Aa, Ab, and D, covering stations S2 to S14, as identified in previous studies (Magalhaes et al., 2016; Tchilibou et al., 2022; Assene et al., 2024). Stations S19 to S21 were positioned in less energetic IT generation areas at site E, while stations S24 and S25 were located outside the influence of the IT fields (site G). Stations were distributed across different areas, including the shelf (e.g., S4, S9, and S19), the shelf-break (e.g., S3, S6, and S10), and the open ocean (e.g., S14, S24, and S20).

Vertical Displacement, homogeneous layers

The results revealed that, over a semi-diurnal tidal cycle, relevant amplitudes of vertical displacements (up to 60 m in length) and pronounced step-like structures (up to 40 m thick) were observed along transects Aa and Ab. In contrast, smaller and thinner structures were identified along other transects, such as E. These

differences are likely related to the propagation of ITs, which induce vertical displacements at tidal frequencies and promote mixing by creating homogeneous layers visible as step-like features in the density structure. The isopycnal displacements and step-like structures observed within the pycnocline are consistent with findings from other IT regions (e.g., Stansfield et al., 2001; Simpson and Sharples, 2012; Bordois, 2015; Koch-Larrouy et al., 2015; Zhao et al., 2016; Bouruet-Aubertot et al., 2018; Xu et al., 2020). Furthermore, IT propagation appears to have stronger energy along transects Aa and Ab compared to others, consistent with prior modeling studies (Tchilibou et al., 2022; Assene et al., 2024).

Direct measurements of dissipation rate

Dissipation rates measured with the VMP ranged from between [10^{-10}, 10^{-5}] W kg^{-1} below the XLD, spanning from the continental shelf to the open ocean. The XLD was found to be considerably larger than the MLD at all stations, except at S8, S10, and S25. This is consistent with regions exhibiting strong subsurface shear, such as the equatorial ocean and western boundary current areas (Noh and Lee, 2008). The exception observed at other stations may reflect larger mixing events that were not captured by the VMP measurements.

The highest dissipation rates, within [10^{-6}, 10^{-5}] W kg^{-1}, were observed primarily at generation sites Aa, Ab, and D (e.g., at stations S6, S10, and S3). Slightly lower but still substantial dissipation rates, ranging from 10^{-8} to 10^{-7} W kg^{-1}, occurred a few kilometers (~40 km) from these generation sites (e.g., at S11 and S7), along IT pathways (e.g., at S12, S13, and S20), and even in regions farther from IT influence (e.g., at S24). Interestingly, dissipation rates were higher within [10^{-7}, 10^{-6}] W kg^{-1} in the open ocean, such as at station S14, located ~230 km from generation site Aa, as summarized in Fig. 9.

Similarly, the vertical eddy diffusivity coefficient, ranging from 10^{-3} to 10^{-1} m^2 s^{-1}, was highest at the shelf-break (at stations S3, S5, and S10), Away from the shelf-break, diffusivity values were lower but still substantial, within [10^{-4}, 10^{-3}] m^2 s^{-1} (e.g., at S2, S7, and S11).

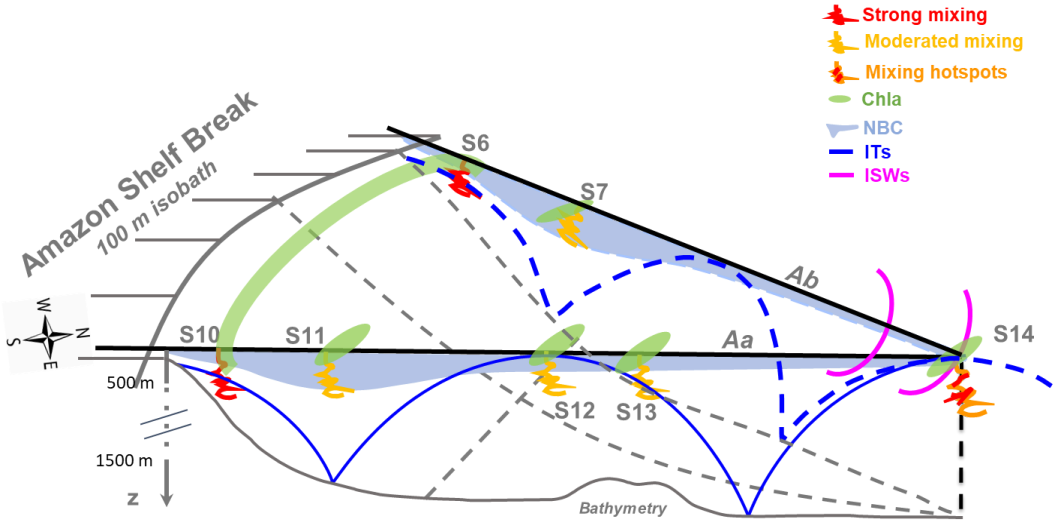

Figure 9: summary diagram illustrating the key processes driving mixing along the AMAZOMIX transects (e.g., Aa and Ab). At IT generation sites (e.g., S6 and S10), mixing rates are stronger, with ITs contributing around 65%, compared to mean circulation (NBC). Along IT pathways (e.g., S7 and S11), mixing decreases but remains notable, driven by nearly equal contributions from ITs and mean circulation. A key observation is the increased mixing ~ 230 km from two distinct IT generation sites at the shelf break. This hotspot at S14 coincides with the surfacing of IT rays from different sites and the presence of ISWs, suggesting that constructive interference of IT rays may generate ISWs, amplifying mixing at S14.

In comparison, in other regions, dissipation rates measured by similar VMP instrument are found between [10^{-7}, 10^{-5}] W kg^{-1} in the IT generation zone of Halmahera Sea, Indonesia (Koch-Larrouy et al., 2015; Bouruet-Aubertot et al., 2018), of Kaena Ridge, Hawaii (Klymak et al., 2008) and off the Changjiang Estuary (Yang et al. 2020). Whereas it is [10^{-10},10^{-8}] $W.kg^{-1}$ along the IT path in the Southern Ocean (Gille et al., 2012) and in Halmahera Sea (Bouruet-Aubertot et al., 2018). Direct estimates of dissipation are almost [10^{-11}, 10^{-10}] W kg^{-1} far from IT influence (Koch-Larrouy et al., 2015; Bouruet-Aubertot et al., 2018) or under the influence of geostrophic current (Takahashi and Hibiya, 2019).

Our mixing coefficients are consistent with, the annual mean between [10^{-4}, 10^{-3}] m^2 s^{-1} of Ffield and Gordon (1992) or Koch-Larrouy et al. (2007), and aligned with others previous studies using the microstructure data (e.g. Tian et al., 2009; Koch-Larrouy et al., 2015; Bouruet-Aubertot et al., 2018; Xu et al., 2020), or modeling results (e.g. Koch-Larrouy et al., 2007).

This crucial vertical eddy diffusivity close enough to the surface along the IT paths may play a role in modulating heat (e.g., Assene et al., 2024) and chlorophyll content (de Macedo et al., 2023; M'Hamdi et al., 2024; in preparation) observed off the Amazon shelf.

Our study also found the highest dissipation rates at stations S3 and S5 of [10^{-6},10^{-4}] W kg^{-1} on the Amazon shelf , increasing near the bottom boundary layer. These findings compare well with values reaching up to 10^{-9} W kg^{-1} within a kilometer of the seabed in the Southern Ocean (Sheen et al., 2013) and up to 10^{-6} W kg^{-1} within a few meters from bottom topography off the Changjiang Estuary (Yang et al. 2020). This may indicate the presence of an active bottom boundary layer. Thus, kinetic energy of bottom flow was estimated using friction velocity, that was computed from total velocity averaged over the bottom-most 15 m for shallow stations. It showed bottom friction energy stronger between 16-35 J m^{-2} at S3 and S5 mainly and lower (< 3 J m^{-2}) in the other stations on shelf (e.g., at S8). These results are smaller but still important on the Amazon shelf and comparable to values (517 kJ m^{-2}) in the Drake Passage region (on the continental slope) of the Southern Ocean (Laurent et al., 2012). The bottom mixing at S3 and S5 can indirectly exert a control on pycnocline mixing on the Amazon shelf (Inall et al., 2021).

Contribution of Background circulation and ITs to mixing

Mean baroclinic current shear

Another important aspect addressed in this study was quantifying the contributions of different processes to the observed heterogeneous mixing.

First, the mean baroclinic current (BC) was considered as a proxy for the background circulation. The BC was predominantly structured into a northwestward surface flow and a southeastward subsurface flow along the IT pathways. The strong surface flow toward the northwest is associated with the North Brazil Current (NBC), which originates from the northeastern coast of Brazil (e.g., Bourlès et al., 1999) and propagates along the Amazon shelf-break (e.g., at stations S7, S10, S11, S14, and S24). Conversely, the southeastward subsurface flow observed at stations such as S7 and S11 might result from NBC instability or the presence of a countercurrent at depth (Dossa et al., 2024, in preparation). At site E, the flow reversal observed at S21 - characterized by a southeastward surface flow and a northwestward subsurface flow - was located inside of the outer path of the Amazon plume. This reversal could be related with the influence of AWL formed by continental inputs (Prestes et al., 2018).

Both baroclinic flows demonstrated a significant potential for shear instability, with vertical shear ranging from 10^{-5} to 10^{-3} s^{-2} off the Amazon shelf. The shear associated with the NBC was particularly pronounced around the pycnocline (between 40 and 200 m depth) at sites Aa, Ab, and G (e.g., at S6, S7, S10, S11, S14, and S24). At site E, the shear instability was stronger (> 2.5 x 10^{-4} s^{-2}) at the base of the pycnocline (e.g., at S20), potentially associated with NBC retroflection near [5–6°N, 50°W] during the fall season (Didden and Schott, 1993). The higher BC shear observed at S21, where flow direction reversals occurred, could be associated with the presence of a subsurface cyclonic eddy (Dossa et al., 2024, in preparation).

ITs shear

Second, the baroclinic tidal current was extracted from the total baroclinic current, revealing significant semi-diurnal (M2) component signals around the pycnocline. These signals, characterized by higher tidal modes (3-5), were more pronounced at generation and propagation sites Aa and Ab (e.g., at S6, S10, and S14) compared to other sites. The tidal shear within the pycnocline layer (80-120 m) is consistent with the observed IT signal patterns and large vertical displacements. It was stronger, reaching up to 10^{-3} s^{-2}, near the generation sites Aa and Ab (at S6 and S10) and in the open ocean at S14. Further from the generation sites (e.g., at S7, S11, and S20), the IT shear was smaller but still notable (reaching up to 10^{-4} s^{-2}). This highlights the significant role of ITs in driving mixing processes, particularly within the pycnocline, where strong vertical shears were observed near the shelf-break compared to regions far away. Outside the IT fields, such as at S24, the persistent high vertical shear near the bottom topography could be attributed to the active bottom boundary layer (Inall et al., 2021).

IT/BC ratio

Both IT and BC shear contribute to mixing, with their relative dominance varying across sites. Near the generation sites on the shelf-break, IT shear dominated the IT/BC shear ratio, such as at S6 (61.44/38.56 %), S10 (65.82/34.18 %), and S21 (58.55/41.45 %). Along the IT paths, the contributions were nearly equal (~50/50 %) at locations farther from the generation sites (e.g., at S20, S7, S11, and S13), except at S14 in the open ocean, where IT shear remained dominant (58.50/41.50 %). These findings align with the presence of ITs at generation sites Aa, Ab, and E (Tchilibou et al., 2022; Assene et al., 2024) and the stronger energy associated with NBC cores, particularly at S7 and S11.

These results are consistent with previous studies that identified strong tidal shear near IT generation sites, such as the Halmahera Sea (Bouruet-Aubertot et al., 2018), the Changjiang Estuary (Yang et al., 2020), the northwest European continental shelf seas (Rippeth et al., 2005), and the southern Yellow Sea (Xu et al., 2020).
The most relevant finding of this study was the relative increase in mixing within the pycnocline layer, observed at S14 in the open ocean, far from the IT generation sites.

Discussion on the strong mixing at S14

Along the IT paths, elevated remote dissipation rates (within [10^{-7}, 10^{-6}] W kg^{-1}) were identified ~ 230 km from the shelf-break at S14.
This region is well known for intense IT dissipation, as shown by a realistic model (Tchilibou et al., 2022; Assene et al., 2024), and for the highest occurrences of ISWs generated by ITs (Fig. 1a; de Macedo et al., 2023), with large-amplitude ISWs exceeding 100 m clearly visible in satellite records (Brandt et al., 2002).
At station S14, where relative mixing increases, IT rays surfacing from two distinct IT generation sites coincide with the appearance of ISWs and mark the location where the NBC vanishes.
This region of wave-wave interactions can lead to the constructive interference of IT rays, potentially facilitating the emergence of higher tidal modes (New & Pingree, 1992; Silva et al., 2015; Barbot et al., 2022; Solano et al., 2023). These higher modes, in turn, could enhance the generation of nonlinear ISWs (e.g., Jackson et al., 2012) and contribute to the elevated dissipation rates (Xie et al., 2013), as observed at this station.
Moreover, IT interactions with baroclinic eddies may also contribute to turbulent dissipation (Booth and Kamenkovich, 2008), particularly in this area of pronounced eddy activity. However, no repeated AMAZOMIX stations observed during a tidal period were enclosed by mesoscale eddy activity, except potentially around site E, where possible evidence of a subsurface eddy was detected at S21 (Dossa et al., 2024, in preparation).
Future studies are needed to unravel the intricate interplay among these processes. The data collected during the AMAZOMIX cruise will provide a guide for improving our understanding and advancing parameterizations for modeling studies.

"

Line 426: "… It showed bottom FICTION"; I think you mean "bottom friction"?

R: Thanks for your remarks. We have rewritten it in line 500 of the revised manuscript, as shown in your previous comment.

In Figure 7 the legend for NBC is given, but it is not drawn in Figure 7.

R: Thanks for your comments. We have updated Figure 9 of revised manuscript as shown below in figure RC3.3.

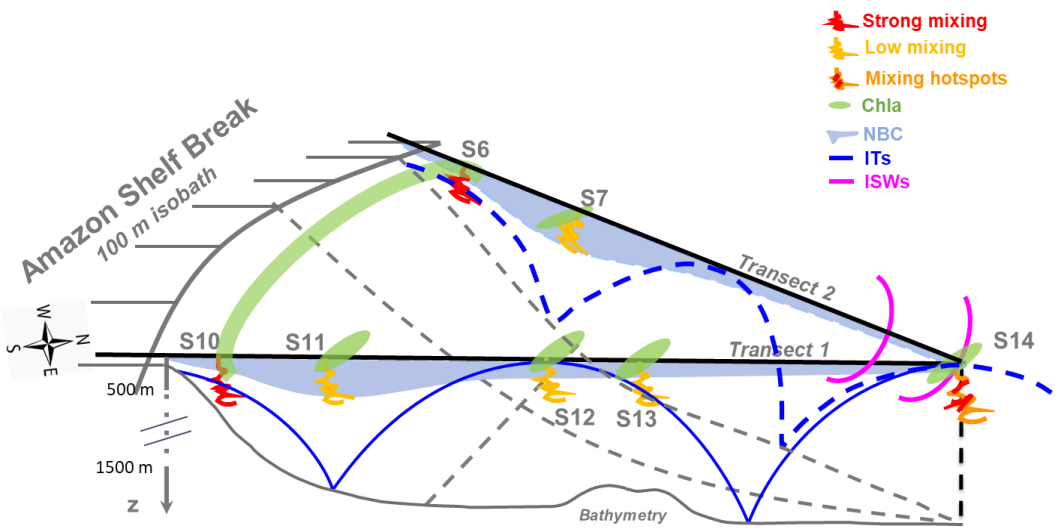

Figure RC3.3: summary diagram illustrating the key processes driving mixing along the AMAZOMIX transects (e.g., Aa and Ab). At IT generation sites (e.g., S6 and S10), mixing rates are stronger, with ITs contributing around 65%, compared to mean circulation (NBC). Along IT pathways (e.g., S7 and S11), mixing decreases but remains notable, driven by nearly equal contributions from ITs and mean circulation. A key observation is the increased mixing ~ 230 km from two distinct IT generation sites at the shelf break. This hotspot at S14 coincides with the surfacing of IT rays from different sites and the presence of ISWs, suggesting that constructive interference of IT rays may generate ISWs, amplifying mixing at S14.

Line 446: “This relative diminution….”.; can you use another word for “diminution” that is more common in literature? Perhaps the word “decrease” suits what the authors want to say?

R: Thanks for your remarks. We have rewritten it in lines 538-549 of the revised manuscript, as shown in your previous comment.

Line 471: “The really new aspect raised in this study…”; Please avoid writing “The really new”. Something is either new or “not new”.

R: Thanks for your remarks. We have rewritten it in lines 548-549 of the revised manuscript, as shown in your previous comment.

Line 483: “ITs disintegrate into a package of ISWs events…”; Please use the word “packet” for ISWs because this is what became acknowledged in the literatute for groups of internal wave trains.

R: Thanks for your remarks. We have rewritten it in lines 551-566 of the revised manuscript, as shown in your previous comment.

Line 510: “…, ITs act as an important supplier of nutrient into….”; please use plural for “nutrients”.

R: Thanks for your remarks.

Ultimately, we decided to remove and reserve all sections on “Nutrients fluxes” for a separate paper in progress.